Oxygen defects in amorphous Al_2O_3: A hybrid functional study

Zhendong Guo,[1, a)] Francesco Ambrosio,[1] and Alfredo Pasquarello[1]
Chaire de Simulation à l'Echelle Atomique (CSEA), Ecole Polytechnique Fédérale de Lausanne (EPFL), CH-1015 Lausanne, Switzerland

(Dated: 15 July 2016)

The electronic properties of the oxygen vacancy and interstitial in amorphous Al_2O_3 are studied via *ab initio* molecular dynamics simulations and hybrid functional calculations. Our results indicate that these defects do not occur in amorphous Al_2O_3, due to structural rearrangements which assimilate the defect structure and cause a delocalization of the associated defect levels. The imbalance of oxygen leads to a nonstoichiometric compound in which the oxygen occurs in the form of O^{2-} ions. Intrinsic oxygen defects are found to be unable to trap excess electrons. For low Fermi energies, the formation of peroxy linkages is found to be favored leading to the capture of holes. The relative +2/0 defect levels occurs at 2.5 eV from the valence band.

PACS numbers: 61.20.Ja,71.15.-m,71.10.-w

Defects in amorphous alumina (a-Al_2O_3) may impact the performance of this material as gate dielectric in metal-oxide semiconductor (MOS) technology.[1–5] For this reason, native defects in Al_2O_3 have been the subject of extensive experimental and theoretical investigations aiming at verifying the presence of deep-level traps in the dielectric.[6–21] The vast majority of theoretical studies performed so far have focused on crystalline phases of Al_2O_3. However, Al_2O_3 in MOS devices is usually deposited via atomic layer deposition, which results in an amorphous phase with electronic properties differing considerably from those of crystalline phases.[21–24] Furthermore, the experimental characterization of defect states in a-Al_2O_3 has led to conflicting interpretations. The oxygen vacancy has been invoked as an electron trap in oxygen-deficient a-Al_2O_3 films on the basis of electron energy loss, photoluminescence, and capacitance measurements, and this suggestion has received support from theoretical studies based on density-functional-theory calculations.[6,21] At variance, Århammar *et al.*[7] synthesized a-Al_2O_3 via physical vapour deposition and investigated the defect states in the gap using X-ray absorption and resonant inelastic scattering techniques. Supplementing their experimental results with computational studies, they assigned the observed defect states to peroxy linkages between two oxygen atoms (O-O) rather than to oxygen vacancies.

In order to elucidate the nature of oxygen-related defects in a-Al_2O_3, we here investigate the structural and electronic properties of oxygen vacancies (V_O) and interstitials (O_i) in a-Al_2O_3 through *ab initio* molecular dynamics (MD) simulations and hybrid functional calculations. We find that structural rearrangements in the amorphous can assimilate oxygen vacancies in the +2 charge state and oxygen interstitials in the −2 charge state removing any electronic state from the band gap. While excess electrons cannot be trapped by intrinsic oxygen defects, the presence of excess holes results in the formation of peroxy linkages, with defect states in the band gap at 2.5 eV from the valence band.

All the calculations are carried out with the freely available `CP2K` suite of codes,[25] which is based on the use of atomic basis sets and of a plane-wave expansion for the electron density. Analytical Goedecker-Teter-Hutter pseudopotentials[26] are used to account for core-valence interactions. We use a triple-ζ correlation-consistent polarized basis set[27] for O atoms, and the shorter range molecularly optimized double-zeta basis set with one polarization function[28] for Al atoms. For the plane-waves, a cutoff of 500 Ry is employed. The sampling of the Brillouin zone is achieved at the sole Γ-point, as justified by extensive convergence tests.[29] Structural relaxations and MD simulations are carried out with the Perdew, Burke, and Ernzerhof (PBE) functional.[30] In order to overcome the band gap underestimation associated with the use of the PBE, the electronic properties are finally evaluated with the functional proposed by Heyd, Scuseria, and Ernzerhof (HSE).[31,32] We set the fraction of Fock exchange to $\alpha = 0.45$, as this value has been found to reproduce the experimental band gap of α-Al_2O_3.[29] The range-separation parameter is kept fixed at its original value, $\mu = 0.11$ bohr^{-1} (Ref. 32), to ensure the accuracy of the hybrid functional.[33] We perform all HSE calculations using the auxiliary density matrix method.[34] With the present setup we indeed reproduce the experimental band gap of 9.13 eV α-Al_2O_3 (Ref. 35), in accord with the result achieved with a plane-wave scheme.[29] As a further test, we consider the O_2 molecule, for which our HSE calculations yield a binding energy of 5.02 eV and an equilibrium bond length of 1.20 Å, in good agreement with their experimental counterparts (5.12 eV, 1.21 Å).[36]

The formation energy $E_f[X^q]$ of an isolated defect X with charge state q can be expressed as a function of the Fermi energy ε_F, defined with respect to the valence band maximum (VBM) ε_v of the bulk system:[37,38]

$$E_f[X^q] = E_{tot}[X^q] + E^q_{corr} - E_{tot}[bulk] - \sum_i n_i\mu_i + q[\varepsilon_F + \varepsilon_v + \Delta\upsilon_{0/b}], \quad (1)$$

where $E_{tot}[X^q]$ is the total energy of the supercell with a defect X in the charge state q, $E_{tot}[bulk]$ the total energy of bulk a-Al_2O_3, n_i the number of added or subtracted atoms of the species i needed to create the defect X, and μ_i the respective chemical potential. The chemical potential of oxygen μ_O is here set to half the energy of an oxygen molecule. The potential alignment term $\Delta\upsilon_{0/b}$ accounts for the potential shift between the bulk and the neutral defect calculation.[38] Finally,

a)Electronic mail: zhendong.guo@epfl.ch

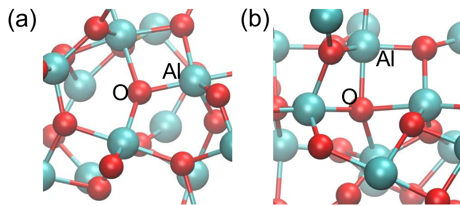

FIG. 1. Representation of (a) a threefold and (b) a fourfold O atom in a-Al_2O_3, prior to vacancy formation.

E^q_{corr} is a finite-size electrostatic correction related to the use of periodic boundary conditions.[38,39] In this work, a defect level is defined as a thermodynamic charge transition level $\varepsilon(q/q')$, corresponding to the specific value of ε_F for which the formation energies in the charge states q and q' coincide.

For a-Al_2O_3, we use an atomistic model structure generated previously through *ab initio* molecular dynamics.[29] The model contains 64 Al and 96 O atoms in an orthorhombic supercell with sides of 11.5, 11.2, and 12.8 Å, corresponding to a mass density of 3.29 g/cm^3, which falls within the experimental range (3.05 – 3.65 g/cm^3).[40–42] Structural properties such as radial distribution functions and coordination numbers also agree well with the experimental characterization.[29] Furthermore, the HSE band gap of this model of a-Al_2O_3 is 6.67 eV, in agreement with experimental values (6.1-7.0 eV).[43–45]

We first focus on the oxygen vacancy, which is found to be an important defect in crystalline Al_2O_3, as well as in numerous other oxides.[46–49] In our calculations, V_O is created by directly removing an O atom from the pristine bulk a-Al_2O_3 model. For removal, we consider five threefold and five fourfold coordinated O atoms (Fig. 1), yielding a distinct defect model for each case upon full structural relaxation. We do not find significant differences among these ten models. The relative energies of the various charge states are illustrated in Fig. 2(a) for the most stable V_O model. As for crystalline oxides,[8–12] the neutral and the +2 charge states are the most stable ones with a +2/0 charge transition level occurring in the band gap of a-Al_2O_3 at ∼5 eV from the VBM.

To investigate the stability of the neutral oxygen vacancy (V^0_O), we then carry out an annealing cycle using *ab initio* molecular dynamics. Through the use of a Nosé-Hoover thermostat,[50,51] the defect system is first equilibrated at 2000 K for 8 ps and then progressively cooled down to 800 K over a period of 8 ps, corresponding to a cooling rate of 150 K/ps. Other tested cooling rates (100, 200, 300 K/ps) produce final structures of equivalent total energy. We here use a high annealing temperature to accelerate the transition of energy barriers in the structural relaxation around the defect in order to restrain the process to time scales that can be afforded in MD simulations. To monitor the total energy during the evolution, the system is fully relaxed from MD configurations at regular intervals showing that a stabilization of almost 5 eV is achieved through the annealing cycle [Fig. 2(e)]. The evolution is continued until the total energy has clearly reached a plateau value. Recalculation of the defect energies in the various charge states reveals that the charge state +2 now dominates throughout the band gap [Fig. 2(b)]. This stabilization is

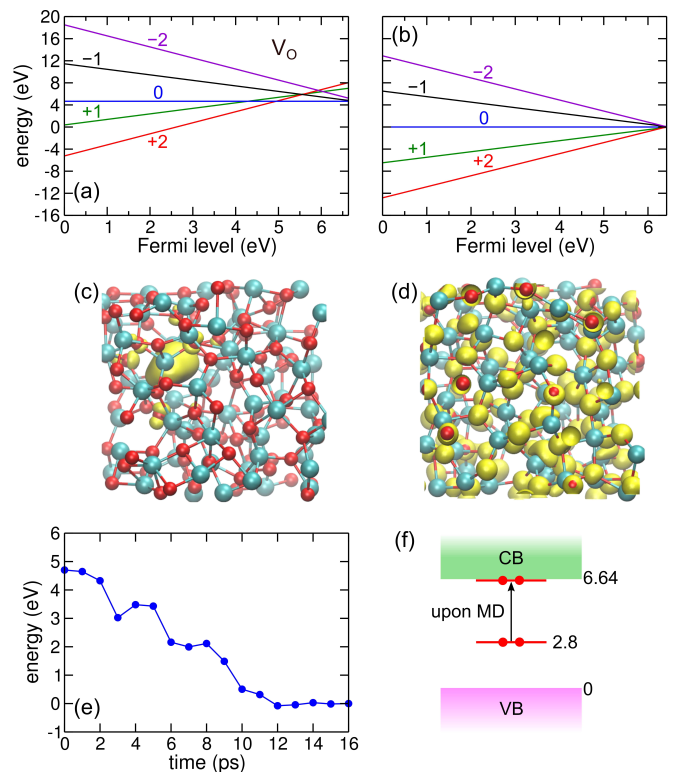

FIG. 2. Relative energies of a-Al_2O_3 upon removal of one O atom, (a) before and (b) after MD annealing. The energies are referred to the energy of the neutral defective system after MD simulation. The extent of the defect state upon the removal of one neutral O atom is illustrated (c) before and (d) after the MD simulation; (e) total energy during the annealing cycle of the neutral O vacancy, obtained by full structural relaxation from configurations occurring during the MD evolution; (f) corresponding evolution of the occupied single-particle energy level of the system upon MD annealing.

accompanied by a complete disappearance of the void resulting from O removal. Interestingly, even the doubly-occupied localized electronic state associated to the vacancy [Fig. 2(c)] has evolved to a delocalized state [Fig. 2(d)], with a concurrent shift of its single particle level from 2.8 eV above the VBM to the conduction band edge [Fig. 2(f)]. Starting from the oxygen vacancy in the +2 charge state, we observe that the localized unoccupied single particle level similarly disappears upon annealing. These results indicate that the vacancy is completely assimilated by the amorphous structure, a property which has previously also been observed for O vacancies in amorphous HfO_2.[48] Since any signature of defect localization has vanished, the use of defect formation energies as defined in Eq. (1) is inappropriate and the energies in Fig. 2 have been referred to the neutral configuration after annealing. The stability of the +2 charge state and the occurrence of delocalized electrons in the neutral charge state indicate that oxygen removal corresponds to the removal of an O^{2-} ion, whereby the amorphous is turned into a defect-free substoichiometric oxide, a-$Al_2O_{3-\delta}$. Thus, unlike in crystalline phases, the oxygen vacancy cannot serve as an electron trap in a-Al_2O_3. The oxygen deficiency results in a release of elec-

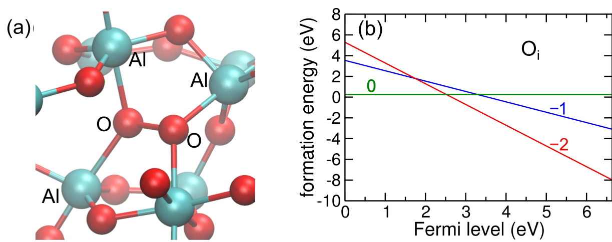

FIG. 3. (a) Representation of the O-O peroxy linkage formed upon the insertion of an interstitial O (O_i) in a-Al_2O_3; (b) formation energy of O_i in various charge states as a function of Fermi energy. The chemical potential of oxygen is set to half the energy of an oxygen molecule.

trons which are likely to be captured by extrinsic defects, e.g. N and C impurities.[52]

Next, we investigate the interstitial oxygen (O_i) in a-Al_2O_3. To determine a suitable location, we carry out a Voronoi analysis which provides us with the position and size of the voids.[53] In consideration of the oxygen ionic radius, we select ten voids with radii ranging between 1.7 and 2.5 Å. For each selected void, we insert an O atom and carry out MD at a target temperature of 1000 K for a duration of 3 ps. This process is repeated for 3 different charge states: 0, -1, and -2. Structural configurations at simulation times of 1, 1.5, 2, 2.5, and 3 ps are sampled from every MD trajectory and then structurally relaxed. Among those configurations, only the lowest-energy one is kept for further investigation, resulting in 10 models for each charge state. During the MD runs, the structural rearrangement induced by the defect is accompanied by a general relaxation of the amorphous structure. In order to ensure that the defect formation energy is not affected by this effect, we adopt a cycling procedure, as proposed earlier for the study of defects in amorphous systems.[48] In this procedure, we first remove the O_i from its relaxed configuration and relax the resulting structure. Hence, we reinsert the defect and relax the structure again. The cycling is continued until the total-energy difference $E_{tot}[X^q] - E_{tot}[\text{bulk}]$ appearing in Eq. (1) converges.

In the charge state -2, the inserted O^{2-} ion is found to be either threefold or fourfold coordinated (Fig. 1), being thus indistinguishable from regular oxygen configurations in pristine a-Al_2O_3. The same structural configurations are encountered for O^-. In the neutral charge state, we systematically observe the formation of an O-O peroxy linkage with an average bond length of 1.51 Å [Fig. 3(a)]. We verify that the formation of this linkage is robust against further structural relaxation at the HSE level. The occurrence of O-O linkages is consistent with NEXAFS and EELS experiments.[7] In Fig. 3(b), we show the formation energy diagram of O_i in a-Al_2O_3. The neutral and -2 charge states are the most stable charge states with a $0/{-2}$ charge transition level at 2.5 eV above the VBM. The charge state -1 is metastable. The formation energies in Fig. 3 refer to the most stable model structures, but they differ by less than 0.3 eV from the average obtained over the set of ten model structures that we have considered for each charge state.

Since extra or missing O atoms in a-Al_2O_3 generally appear

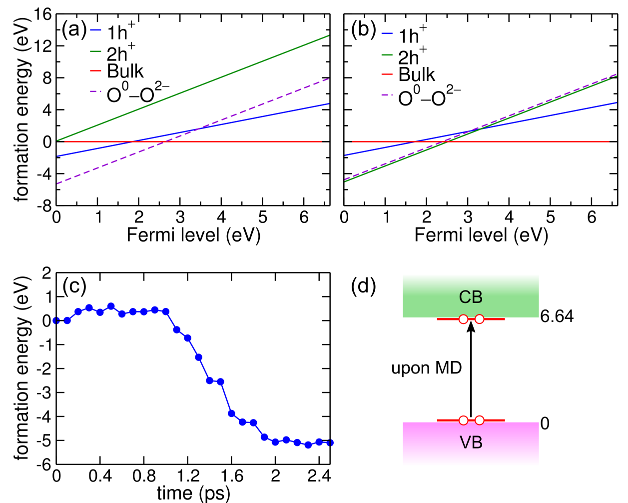

FIG. 4. Formation energies of one and two holes in a-Al_2O_3 as a function of ε_F with respect to VBM, (a) before and (b) after MD simulations. The formation energy difference between the charge states 0 and -2 for the O_i, $E_f[O_i^0] - E_f[O_i^{2-}]$, is reported for comparison; (c) total energy during the annealing cycle of the amorphous system with two holes, obtained by full structural relaxation from configurations occurring during the MD evolution; (f) corresponding evolution of the unoccupied single-particle energy level of the system upon MD annealing.

in the form of O^{2-} ions, we investigate whether the formation of an O-O peroxy linkage observed in the case of the neutral O_i could be induced by electron depletion. To this aim, we introduce one or two holes (h^+) in the pristine a-Al_2O_3 model, and apply the same computational procedure employed for O_i. Before MD simulation [Fig. 4(a)], the single hole is found to be bound with a binding energy of $\sim$2 eV, while the system with two holes does not lead to any localized state. However, upon MD simulations, the energy diagram changes considerably [Fig. 4(b)]. In particular, the system with two holes undergoes significant stabilization [Fig. 4(c)] with its unoccupied single particle state moving from the valence band all the way to the conduction band [Fig. 4(d)]. These changes result form the rearrangement of the amorphous structure leading to the formation of an O-O peroxy linkage. In view of these observations, the neutral state of O_i should be interpreted as the occurrence of an O^{2-} ion with two independent holes. Indeed, this interpretation is also supported by the calculated formation energies. As illustrated in Fig. 4(b), we find that the stabilization energy upon the formation of the peroxy linkage is the same when the holes are introduced in the pristine a-Al_2O_3 or in a-Al_2O_3 with an additional O^{2-} ion, i.e. $E_f[O_i^0] - E_f[O_i^{2-}] = E_f[2h^+]$. We remark that the formation of a O-O linkage is a reversible process. When the two missing electrons are returned, they first go into the conduction band but eventually their energy level returns to the valence band upon structural rearrangements which break the O-O bond. Hence, we conclude that the formation of the peroxy linkage is a direct consequence of electron depletion and that the associated charge transition level at 2.5 eV corresponds to the

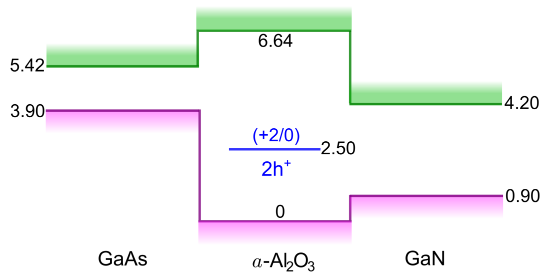

FIG. 5. Position of +2/0 hole trapping level in a-Al_2O_3 with respect to the band edges of GaAs and GaN. The band alignment is taken from photoemission experiments (Refs. 43–45, and 54).

binding of two holes in pristine a-Al_2O_3.

It is of interest to focus on practical implications for MOS devices based on the Al_2O_3 dielectric. For GaAs/Al_2O_3 interfaces,[43–45] we show in Fig. 5 the position of the calculated charge transition level with respect to the band edges of GaAs. The +2/0 charge transition level of a-Al_2O_3 falls at ∼1.5 eV below the VBM of GaAs. Our study therefore rules out that oxygen-related defects or intrinsic trapping mechanisms in a-Al_2O_3 could cause performance degradation in such MOS devices. At variance, for the band alignment at GaN/Al_2O_3 interfaces,[54] the +2/0 charge transition level lies in the band gap of the semiconductor and the peroxy linkage might constitute a conduction channel for hole leakage in p-type doping conditions.

In conclusion, we investigated the electronic properties of oxygen vacancies and oxygen interstitials in a-Al_2O_3. The structure of a-Al_2O_3 rearranges in such a way that the excess or deficiency of isolated O^{2-} ions show electronic properties which do not differ from those of the pristine material. The oxygen vacancy leads to substoichiometric oxide in which excess electrons are released. Analogously, the presence of excess oxygen induces the generation of holes, which can be bound in the amorphous structure through the formation of peroxy linkages. The associated defect levels lie at ∼2.5 eV from the valence band edge and can thus not lead to device degradation in GaAs-based MOS devices. In contrast, the perfomance of GaN-based MOS devices could be affected as the defect level is found to be at ∼2 eV above the valence band edge of GaN.

We thank Davide Colleoni and Giacomo Miceli for fruitful discussions and for providing the coordinates of the a-Al_2O_3 model generated in Ref. 29. We also thank Claudia Cancellieri for useful interactions. This work has been performed in the context of the National Center of Competence in Research (NCCR) "Materials' Revolution: Computational Design and Discovery of Novel Materials (MARVEL)" of the Swiss National Science Foundation. We used computational resources of CSCS and CSEA-EPFL.

[1] P. Ye, G. Wilk, J. Kwo, B. Yang, H.-J. Gossmann, M. Frei, S. Chu, J. Mannaerts, M. Sergent, M. Hong, K. Ng, and J. Bude, IEEE Electron Device Lett. **24**, 209 (2003).
[2] P. D. Ye, B. Yang, K. K. Ng, J. Bude, G. D. Wilk, S. Halder, and J. C. M. Hwang, Appl. Phys. Lett. **86**, 063501 (2005).
[3] H. Zhao, D. Shahrjerdi, F. Zhu, M. Zhang, H.-S. Kim, I. OK, J. H. Yum, S. I. Park, S. K. Banerjee, and J. C. Lee, Appl. Phys. Lett. **92**, 233508 (2008).
[4] Y. Xuan, Y. Wu, H. Lin, T. Shen, and P. Ye, IEEE Electron Device Lett. **28**, 935 (2007).
[5] P. Kordoš, D. Gregušová, R. Stoklas, K. Čičo, and J. Novák, Appl. Phys. Lett. **90**, 123513 (2007).
[6] T. V. Perevalov, O. E. Tereshenko, V. A. Gritsenko, V. A. Pustovarov, A. P. Yelisseyev, C. Park, J. H. Han, and C. Lee, J. Appl. Phys. **108**, 013501 (2010).
[7] C. Århammar, A. Pietzsch, N. Bock, E. Holmström, C. M. Araujo, J. Grsjö, S. Zhao, S. Green, T. Peery, F. Hennies, S. Amerioun, A. Föhlisch, J. Schlappa, T. Schmitt, V. N. Strocov, G. A. Niklasson, D. C. Wallace, J.-E. Rubensson, B. Johansson, and R. Ahuja, Proc. Natl. Acad. Sci. U.S.A. **108**, 6355 (2011).
[8] M. Choi, A. Janotti, and C. G. Van de Walle, J. Appl. Phys. **113**, 044501 (2013).
[9] M. Choi, J. L. Lyons, A. Janotti, and C. G. Van de Walle, Phys. Status Solidi B **250**, 787 (2013).
[10] L. Gordon, H. Abu-Farsakh, A. Janotti, and C. G. Van de Walle, Sci. Rep. **4**, 07590 (2014).
[11] J. R. Weber, A. Janotti, and C. G. Van de Walle, Microelectron. Eng. **86**, 1756 (2009).
[12] J. R. Weber, A. Janotti, and C. G. Van de Walle, J. Appl. Phys. **109**, 033715 (2011).
[13] H. Li and J. Robertson, J. Appl. Phys. **115**, 203708 (2014).
[14] D. Liu, S. J. Clark, and J. Robertson, Appl. Phys. Lett. **96**, 032905 (2010).
[15] D. Liu, Y. Guo, L. Lin, and J. Robertson, J. Appl. Phys. **114**, 083704 (2013).
[16] K. Xiong, J. Robertson, and S. J. Clark, J. Appl. Phys. **102**, 083710 (2007).
[17] J. Carrasco, J. R. B. Gomes, and F. Illas, Phys. Rev. B **69**, 064116 (2004).
[18] F. Janetzko, R. A. Evarestov, T. Bredow, and K. Jug, Phys. Status Solidi B **241**, 1032 (2004).
[19] K. Matsunaga, T. Tanaka, T. Yamamoto, and Y. Ikuhara, Phys. Rev. B **68**, 085110 (2003).
[20] H. Momida, S. Nigo, G. Kido, and T. Ohno, Appl. Phys. Lett. **98**, 042102 (2011).
[21] B. Shin, J. R. Weber, R. D. Long, P. K. Hurley, C. G. Van de Walle, and P. C. McIntyre, Appl. Phys. Lett. **96** (2010), http://dx.doi.org/10.1063/1.3399776.
[22] Y. Chang, F. Ducroquet, E. Gautier, O. Renault, J. Legrand, J. Damlencourt, and F. Martin, Microelectron. Eng. **72**, 326 (2004).
[23] H. Lin, P. Ye, and G. Wilk, Solid-State Electron. **50**, 1012 (2006).
[24] H. H. Pham and L.-W. Wang, Phys. Chem. Chem. Phys. **17**, 541 (2015).
[25] J. VandeVondele, M. Krack, F. Mohamed, M. Parrinello, T. Chassaing, and J. Hutter, Comput. Phys. Commun. **167**, 103 (2005).
[26] S. Goedecker, M. Teter, and J. Hutter, Phys. Rev. B **54**, 1703 (1996).
[27] T. H. Dunning, J. Chem. Phys. **90**, 1007 (1989).
[28] J. VandeVondele and J. Hutter, J. Chem. Phys. **127**, 114105 (2007).
[29] D. Colleoni, G. Miceli, and A. Pasquarello, Appl. Phys. Lett. **107**, 211601 (2015).
[30] J. P. Perdew, K. Burke, and M. Ernzerhof, Phys. Rev. Lett. **77**, 3865 (1996).
[31] J. Heyd, G. E. Scuseria, and M. Ernzerhof, J. Chem. Phys. **118**, 8207 (2003).
[32] J. Heyd, G. E. Scuseria, and M. Ernzerhof, J. Chem. Phys. **124**, 219906 (2006).
[33] H.-P. Komsa, P. Broqvist, and A. Pasquarello, Phys. Rev. B **81**, 205118 (2010).
[34] M. Guidon, J. Hutter, and J. VandeVondele, J. Chem. Theory Comput. **6**, 2348 (2010).
[35] R. H. French, J. Am. Ceram. Soc. **73**, 477 (1990).
[36] K.-P. Huber, *Molecular spectra and molecular structure: IV. Constants of diatomic molecules* (Springer Science & Business Media, 2013).
[37] A. Alkauskas, P. Broqvist, and A. Pasquarello, Phys. Status Solidi B **248**, 775 (2011).
[38] H.-P. Komsa, T. T. Rantala, and A. Pasquarello, Phys. Rev. B **86**, 045112 (2012).
[39] C. Freysoldt, J. Neugebauer, and C. G. Van de Walle, Phys. Rev. Lett. **102**, 016402 (2009).
[40] Y. Oka, T. Takahashi, K. Okada, and S. Ichi Iwai, J. Non-Cryst. Solids **30**, 349 (1979).

[41]P. Lamparter and R. Kniep, Phys. B **234236**, 405 (1997).
[42]S.-M. Lee, D. G. Cahill, and T. H. Allen, Phys. Rev. B **52**, 253 (1995).
[43]M. L. Huang, Y. C. Chang, C. H. Chang, T. D. Lin, J. Kwo, T. B. Wu, and M. Hong, Appl. Phys. Lett. **89**, 012903 (2006).
[44]J. Ahn, I. Geppert, M. Gunji, M. Holland, I. Thayne, M. Eizenberg, and P. C. McIntyre, Appl. Phys. Lett. **99**, 232902 (2011).
[45]I. Krylov, D. Ritter, and M. Eizenberg, J. Appl. Phys. **117**, 174501 (2015).
[46]J. Robertson, Rep. Prog. Phys. **69**, 327 (2006).
[47]P. Broqvist and A. Pasquarello, Appl. Phys. Lett. **89**, 2904 (2006).
[48]P. Broqvist and A. Pasquarello, Microelectron. Eng. **84**, 2022 (2007).
[49]A. Alkauskas and A. Pasquarello, Phys. Rev. B **84**, 125206 (2011).
[50]S. Nosé, J. Chem. Phys. **81**, 511 (1984).
[51]W. G. Hoover, Phys. Rev. A **31**, 1695 (1985).
[52]M. Choi, J. L. Lyons, A. Janotti, and C. G. Van de Walle, Appl. Phys. Lett. **102**, 142902 (2013).
[53]F. Aurenhammer, ACM Computing Surveys (CSUR) **23**, 345 (1991).
[54]T. L. Duan, J. S. Pan, and D. S. Ang, Appl. Phys. Lett. **102**, 201604 (2013).